VIROLOGICA SINICA 2017, 32 (2): 163–166
DOI: 10.1007/s12250-016-3903-5

LETTER

Characterization of viral entry and infection of quantum dot-labeled grass carp reovirus

Dear Editor,

Reoviruses are non-enveloped icosahedral virions with an outer capsid surrounding their cores, which harbor the 10–12 segmented double-stranded RNA (dsRNA) genome. To date, there are 15 proposed genera in the family *Reoviridae* (King et al., 2012), including *Aquareovirus*. Generally, aquareoviruses are of low pathogenicity in aquaculture. However, grass carp reovirus (GCRV) is a highly pathogenic agent that is capable of causing serious hemorrhagic disease in aquatic animals (Fang et al., 1989; Rangel et al., 1999). Thus, GCRV serves as an ideal model for studying the infection and pathogenesis of aquareoviruses.

Viral infection in host cells is a complex biological process. Tracking virus entry into living cells is a great challenge in the study of the dynamic interactions between viruses and target cells (Brandenburg and Zhuang, 2007). A wide variety of approaches have been developed using fluorophores (such as fluorescent proteins, organic dyes, and nanoparticles) to label viruses for studying real-time virus-cell interactions (Bruchez et al., 1998; Howarth et al., 2005). Compared with conventional organic dyes, inorganic nanoparticle quantum dots (QDs) exhibit many promising features, such as remarkable photostability and brightness with a narrow emission spectrum as well as ultrasensitive, long-term biolabeling (Bruchez et al., 1998; Medintz et al., 2005). To image viral behaviors in host cells, the dynamics of population infection behaviors and interactions between virus and cell organelles have been visualized using QD labeling and advanced microscope technologies (Howarth et al., 2005; Liu et al., 2012; Zhang et al., 2013).

Similar to other reoviruses in the *Spinareovirinae* group of family *Reoviridae*, the structure of GCRV is constructed by a turreted core and outer capsid with an overall diameter of approximately 80 nm. The outer shell of GCRV is composed of two proteins (VP5 and VP7), and the inner capsid is composed of five structural proteins (VP1–VP4 and VP6). Typically, five VP1 molecules compose a turret situated at each five-fold vertice (Fang et al., 2005; Li and Fang, 2013). In this way, VP1 is also a surface protein. Moreover, reoviruses have been reported to enter into cells through a penetration mechanism other than the membrane fusion mechanism commonly used by enveloped viruses (Liemann et al., 2002; Zhang et al., 2010). However, the detailed entry mechanism of non-enveloped virus is poorly understood. As a step toward understanding the entry basis of GCRV pathogenesis, we established a method for specific surface labeling of biotinylated GCRV with QDs and investigated the biological features of QD-labeled GCRV.

In order to realize stable surface labeling of the GCRV outer capsid proteins depicted in Figure 1A, GCRV was propagated in *Ctenopharyngodon idellus* kidney (CIK) cells and purified by ultracentrifugation as previously described (Fang et al., 2008; Yan et al., 2015). The concentrated GCRV particles were incubated with sulfosuccinimidyl-6-biotinamidohexanoate (sulfo-NHS-LC-biotin; Thermo) at 28 °C for 2 h according to the manufacturer's instructions, and the unbound biotinylating agent was removed using a spin desalting column (Thermo). After confirming the proper biotinylation of the three surface proteins (data not shown), the QD labeled-GCRVs (QD-GCRVs) were obtained by incubating biotinylated GCRV with streptavidin-conjugated QDs (SA-QDs) at 25 °C. Next, the QD-GCRVs were purified through gradient centrifugation and examined with an electron microscope, as described previously (Fang et al., 2005; Zhang et al., 2013). As shown in Figure 1B, the band locations of fractions 1 and 2 (F1 and F2) from QD-labeled GCRVs corresponded to the unmodified GCRV gradient F1' and F2', indicating that the general properties of the GCRV particles were not changed by surface labeling with QDs. Further transmission electron microscopy (TEM) observations from negatively stained particles showed that the bands F1' and F2' from the unmodified GCRV gradient were empty particles (also called top components) and intact particles (Figure 1C, 1D) respectively, and clear images of QD-labeled viruses could be easily observed with non-negatively stained particles (Figure 1E). To determine whether bands F1 and F2 contained major viral structural protein components of GCRV, the collected fractions were subjected to SDS-PAGE and confirmed by western blotting analyses using polyclonal antibodies (pAbs) against the viral core frame

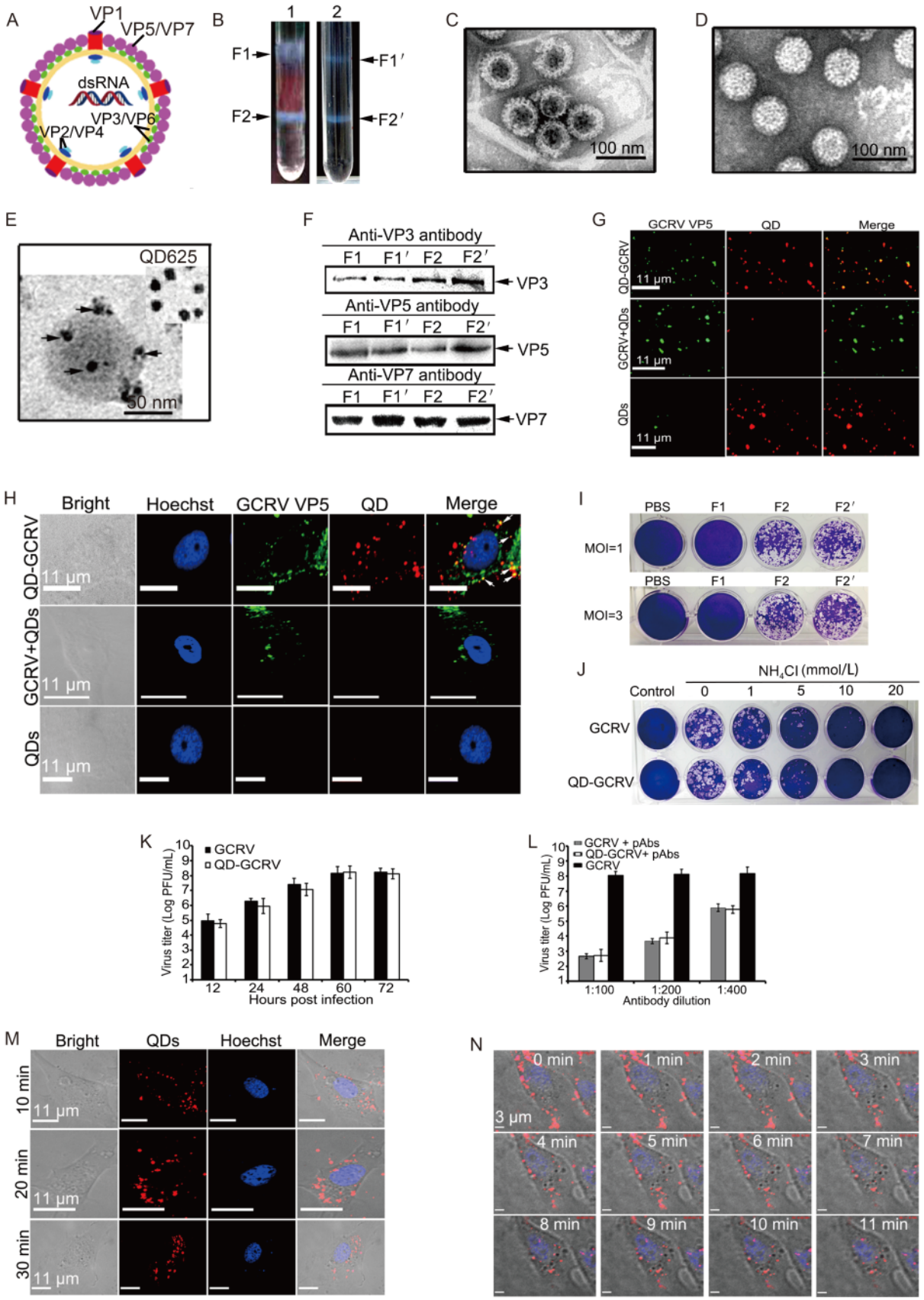
A
VP1
VP5/VP7
dsRNA
VP3/VP6
VP2/VP4
B
1
2
F1
F2
F1′
F2′
C
100 nm
D
100 nm
E
QD625
30 nm
F
Anti-VP3 antibody
F1 F1′ F2 F2′
VP3
Anti-VP5 antibody
F1 F1′ F2 F2′
VP5
Anti-VP7 antibody
F1 F1′ F2 F2′
VP7
G
GCRV VP5
QD
Merge
QD-GCRV
GCRV+QDs
QDs
11 μm
H
Bright
Hoechst
GCRV VP5
QD
Merge
QD-GCRV
GCRV+QDs
QDs
11 μm
I
PBS
F1
F2
F2′
MOI=1
MOI=3
J
NH4Cl (mmol/L)
Control
0
1
5
10
20
GCRV
QD-GCRV
K
GCRV
QD-GCRV
Virus titer (Log PFU/mL)
Hours post infection
12
24
48
60
72
L
GCRV + pAbs
QD-GCRV+ pAbs
GCRV
Virus titer (Log PFU/mL)
1:100
1:200
1:400
Antibody dilution
M
Bright
QDs
Hoechst
Merge
10 min
20 min
30 min
11 μm
N
0 min
1 min
2 min
3 min
4 min
5 min
6 min
7 min
8 min
9 min
10 min
11 min
3 μm

Figure1. Characteristics of the QD-labeled GCRVs. (A) Schematic diagram of GCRV particles. The location of structural proteins is indicated. (B) Ultra-centrifugation images of QD-labeled and unmodified GCRV preparations. Arrowheads indicate the positions of separated bands in each gradient. (C, D) Negatively stained GCRV image from F1' and F2' in tube 2. Empty particle (C), intact virion (D). (E) Unstained QD-GCRV image from F2 in tube 1. Arrowheads in E indicate QD-conjugated GCRV particles. (F) Western blot analysis of major structural protein composition from the bands of purified QD-GCRVs and native particles using polyclonal antibodies against VP3, VP5, and VP7. (G) Fluorescence colocalization assay of the purified QD-GCRV conjugates. Immunofluorescence staining was performed using anti-VP5 antibodies and Alexa 488-labeled donkey anti-mouse IgG (green). QDs are indicated in red. (H) Immunofluorescence assay of QD-GCRV entry in infected CIK cells. VP5 surface protein of GCRV (green) and QD (red) overlapped (yellow), as indicated with white arrowheads. The nucleoli of CIK cells were stained with Hoechst 33342 (blue). GCRV+QDs and QDs served as controls. (I) Plaque formation assays of different GCRV particles. CIK cells were infected with the collected GCRV particles at an MOI of 1 or 3 for 1 h at 28 °C. After adsorption, cells were washed with PBS and incubated in MEM supplemented with 2% FBS at 28 °C for 48 h. The cells were then fixed with paraformaldehyde and stained for analysis. (J) Plaque assays of QD-GCRV in the presence or absence of NH_4Cl. (K) Viral titers were determined by plaque assays. The data shown represent the mean values and standard deviations of the results. Three independent experiments, repeated three times for each sample, were performed. (L) Neutralization of GCRV and QD-GCRV using anti-GCRV polyclonal antibodies. (M) Time-lapse images of QD-GCRVs in CIK cells at different time points after infection. (N) *In situ* real-time images of QD-GCRVs in live cells after performing synchronized infection.

protein VP3 and major surface proteins VP5 and VP7. As shown in Figure 1F, the main core protein VP3 and outer capsid proteins VP5 and VP7 from QD-labeled GCRV preparation were distributed in F1 and F2, corresponding to the molecular weight ranges of unmodified GCRV structural proteins from F1' and F2', consistent with the results reported previously (Fang et al., 2008). These results suggested that the QD-labeled GCRV in band F2 represented intact particles and could be used for further assays.

To determine whether SA-QD properly bound to the surface protein of biotinylated GCRV, QD-GCRVs were seeded onto polylysine-coated coverslips and immunostained with anti-VP5 pAb. As shown in Figure 1G, most of the QD-GCRVs colocalized with VP5. As a control, unbiotinylated GCRV with QDs (GCRV+QDs) and free QDs showed negligible fluorescence in all cases, thus ruling out interference from nonspecific binding. These results indicated that the QD-GCRVs could specifically bind with anti-VP5 pAb, suggesting that the surface proteins of GCRV were properly conjugated with QDs and that the QD images could represent GCRV particles.

To prove whether the QD signals in modified GCRVs could be tracked during entry into cells, the CIK cells were adsorbed with QD-GCRVs at 4 °C for 30 min and then incubated at 28 °C for 15 min. In addition, GCRV+QDs and QDs served as parallel controls. After washing with PBS, infected cells were fixed with paraformaldehyde and then immunostained with pAb against VP5. Results showed that QD-GCRV was colocalized with VP5 during cell entry, whereas no similar colocalization was found in QDs- and GCRV+QDs-infected cells (Figure 1H). These results indicated that the entry properties of the modified GCRV were not significantly altered by QD conjugation and that QD-GCRVs could be used for cell tracking during viral entry.

The inhibitor NH_4Cl can specifically block the reovirus entry pathway (Sturzenbecker et al., 1987; Yan et al., 2015); thus, to further elucidate whether the modified GCRV retained its native particle properties, we assessed the effects of the inhibitor on QD-GCRV infectivity using plaque assays. As shown in Figure 1I, typical plaques in infected CIK cells were observed with intact QD-GCRVs at different multiplicities of infection (MOIs), showing a pattern similar to that of unmodified GCRV. In contrast, no plaques were observed with empty particle infection. In addition, the plaque formation of QD-GCRVs was inhibited by increasing the concentration of NH_4Cl during viral infection, similar to native GCRV (Figure 1J). These results revealed that QD-labeled GCRV could enter cells and initiate infection, similar to native GCRV. To confirm the biological activity of QD-GCRV, virus production at different times after infection and its neutralization capacity with different dilutions of anti-GCRV pAbs were also evaluated. The results showed that the titer of QD-GCRV in infected cells could reach 10^8 pfu/mL at 60 h post-infection (Figure 1K), while the viral yield was reduced by about 4 log after infection of the cells with a mixture of QD-GCRV pre-incubated with anti-GCRV antibody (1 : 200 dilution), as previously reported (Shao et al., 2011), and similar results were also obtained with unmodified GCRV (Figure 1L). The data suggest that there were no significant differences in viral production and neutralization ability between the QD-labeled and unlabeled viruses.

To test whether the QD-GCRV could facilitate real-time viral tracking during entry into host cells, the CIK

cells were incubated with QD-GCRVs at 4 °C for 30 min to allow synchronized virus adsorption and then maintained in Eagle's minimum essential medium at 28 °C. At the indicated times post-infection, the infected cells were fixed for fluorescence microscopy observation. As shown in Figure 1M, many QD-GCRVs (red fluorescent dots) localized near the cell membrane could be detected at 10 min postinfection and then moved into cytoplasm as infection progressed. At the same time, *in situ* real-time dynamic tracking image in live cells was also conducted using time-lapse confocal fluorescence microscopy. As shown in Figure 1N and Supplementary Movie S1, many QD-GCRVs attached to the cell membrane at the beginning of synchronized infection and were subsequently internalized into the cytoplasm. This result strongly indicated that the photostable QDs had advantages for use as fluorescent probes for virus imaging and that QD-GCRVs were qualified to be used for tracking in live cells.

In order to realize stable virus labeling, the purified GCRV particle was first biotinylated and then conjugated with SA-QDs. Our results indicated that SA-QDs could be specifically conjugated with biotinylated GCRV. In fact, such labeling and related methods have been successfully applied to targeting QDs to surface proteins in living cells and adeno-associated virus (AAV) (Howarth et al., 2005). Further western blot analysis confirmed that the surfacing labeling strategy was effective for obtaining QD-labeled GCRV. Moreover, viral yield and neutralization capacity determination by plaque assays proved that the established labeling approach did not significantly affect viral infectivity and immunogenicity. Using synchronized viral infection, a continuous dynamic tracking image of QD-GCRV entering into live cells was obtained, which could greatly reduce fluorescent noise during tracking (Liu et al., 2012; Zhang et al., 2013). Taken together, our data indicated that GCRV labeled by QDs still maintained its original biological function and that the QD-GCRVs could be used as a promising fluorescent marker to study the molecular mechanisms of viral entry by fluorescence microscopy.

In this study, we characterized a QD-labeled non-enveloped aquareovirus. Our results showed that QD-GCRVs maintained their native particle properties and showed excellent infectivity in host cells. To the best of our knowledge, this is the first study reporting the realization of *in situ* real-time tracking with fluorophores in live cells by utilizing a QD-labeled non-enveloped aquareovirus. Although the QD-GCRV can't track the whole process of viral infection, this approach will provide a promising prospect for further studies of the molecular mechanisms of viral entry into host cells during aquareovirus infection.

FOOTNOTES

This work is supported in part by grants from the National Natural Science Foundation of China (31372565, 31400139) and the State Key Laboratory of Freshwater Ecology and Biotechnology (2013FB05). We also thank the support from "The Core Facility and Technical Support of Wuhan Institute of Virology". The authors declare that they have no conflicts of interest. This article does not contain any studies with human or animal subjects performed by any of the authors.

Suppementary Movie S1 is available on the websites of *Virologica Sinica*: www.virosin.org; link.springer.com/journal/ 12250.

Fuxian Zhang[#], Shicui Yan[#], Hong Guo, Qingxiu Chen, Qin Fang[✉]

State Key Laboratory of Virology, Wuhan Institute of Virology, Chinese Academy of Sciences, Wuhan 430071, China.
#These authors contributed equally to this work.
✉Correspondence:
Phone: +86-27-87198551, Fax: +86-27-87198551,
Email: qfang@wh.iov.cn
ORCID: 0000-0003-4681-0060

Published online: 23 January 2017

REFERENCES

Brandenburg B, Zhuang X. 2007. Nat Rev Microbiol, 5: 197–208.
Bruchez M, Moronne M, Gin P, et al. 1998. Science, 281: 2013–2016.
Fang Q, Ke L, Cai Y. 1989. Virol Sin, 4: 315–319.
Fang Q, Sanket S, Liang YY, et al. 2005. Sci China Ser C, 48: 593–600.
Fang Q, Seng E, Ding Q, et al. 2008. Arch Virol, 153: 675–682.
Howarth M, Takao K, Hayashi Y, et al. 2005. Proc Natl Acad Sci U S A, 102: 7583–7588.
Herniou EA, Arif BM, Becnel JJ, et al. 2012. Virus Taxonomy: classification and nomenclature of viruses: Ninth Report of the International Committee on Taxonomy of Viruses. King AMQ, Adams MJ, Cartens EB, Lefkowitz EJ (eds). Amsterdam: Elsevier.
Li X, Fang Q. 2013. Virol Sin, 28: 318–325.
Liemann S, Chandran K, Baker TS, et al. 2002. Cell, 108: 283–295.
Liu SL, Zhang ZL, Tian ZQ, et al. 2012. ACS Nano, 6: 141–150.
Medintz IL, Uyeda HT, Goldman ER, et al. 2005. Nat Mater, 4: 435–446.
Rangel AA, Rockemann DD, Hetrick FM, et al. 1999. J Gen Virol, 80: 2399–2402.
Shao L, Sun X, Fang Q. 2011. Virol J, 8: 347.
Sturzenbecker L, Nibert M, Furlong D, et al. 1987. J Virol, 61: 2351–2361.
Yan S, Zhang J, Guo H, et al. 2015. J Gen Virol, 96: 1795–800.
Zhang F, Zheng Z, Liu SL, et al. 2013. Biomaterials, 34: 7506–7518.
Zhang X, Jin L, Fang Q, et al. 2010. Cell, 141: 472–482.